

# Elastic behavior of poly(ethylene terephthalate) chains

Jin Chen, Linxi Zhang \*

*Department of Physics, Wenzhou Normal College, Wenzhou 325027, PR China*

Received 21 November 2003; received in revised form 2 June 2004; accepted 10 June 2004

Available online 26 August 2004

## Abstract

The Monte Carlo (MC) method based on the rotational-isomeric-state (RIS) model is adopted in studying the elastic behavior of poly(ethylene terephthalate) (PET) chains in this paper. The mean-square end-to-end distance  $\langle R^2 \rangle$ , the mean-square radius of gyration  $\langle S^2 \rangle$ , and the ratio of  $\langle R^2 \rangle / \langle S^2 \rangle$  all increase with elongation ratio  $\lambda$ . The interior conformations are also investigated through calculating the a priori probability of rotational state in the process of tensile elongation. The radius of gyration tensor  $S$  is introduced here in order to measure the shape of PET chains, and  $\langle L_3^2 \rangle / \langle L_1^2 \rangle$  increases with elongation ratio  $\lambda$ , however, some different behaviors are obtained for  $\langle L_2^2 \rangle / \langle L_1^2 \rangle$ . Here  $L_1^2$ ,  $L_2^2$  and  $L_3^2$  are the eigenvalues of the radius of gyration tensor  $S$  ( $L_1^2 \leq L_2^2 \leq L_3^2$ ). The average energy per repeat unit  $\langle U \rangle$  and the average free energy per repeat unit  $\langle A \rangle$  are also calculated, and we find that the average energy decreases with elongation ratio  $\lambda$ , however, the average free energy per repeat unit increases with elongation ratio  $\lambda$ . Elastic force  $f$ , energy contribution to force  $f_U$ , and entropy contribution to force  $f_S$  are also investigated. Both elastic force  $f$  and entropy contribution to force  $f_S$  increases with  $\lambda$ , however, energy contribution to force  $f_U$  and the ratio  $f_U/f$  decreases with  $\lambda$ . The ratio of  $f_U/f$  is less than zero and almost independent of chain length. The results of these microscopic calculations may explain some macroscopic phenomena of rubber elasticity.

© 2004 Elsevier Ltd. All rights reserved.

**Keywords:** Poly(ethylene terephthalate) chain; Elastic behavior; Monte Carlo method

## 1. Introduction

Rubber elasticity is an important phenomenon in polymer physics. Although the molecular origin of the elastic force in a rubber-like material has been known for a quite some time, the relationship between the deformations at macroscopic and molecular levels has

not been fully understood yet. The earliest elasticity experiments involved stress–strain–temperature relationship, or network “thermoelasticity”, first carried out many years ago, by Gough, back in 1805, and more qualitatively by Joule in 1859 [1–3], and the results implicated entropy decreases as the origin of the restrictive force. This is the important experimental fact that mechanical deformations of rubber-like materials generally occurred at essentially constant volume, so long as crystallization was not induced [2]. In the 1930s, Kuhn, Guch, and Mark first began to develop quantitative theories to study rubber elasticity using the Gaussian chain

\* Corresponding author. Tel.: +86 571 879 53261; fax: +86 571 879 51328.

E-mail address: [lxzhang@hzcnc.com](mailto:lxzhang@hzcnc.com) (L. Zhang).

model [1,2]. Later, non-Gaussian theories have also been developed [4,5], and Abe and Flory put forward the rotational isomeric state (RIS) theory based on the effects of elongation of a polymer chain on the apportionment of its bonds and bond sequences among various RIS [6]. Mark and Curro investigated rubber-like elasticity basis of distribution functions for end-to-end separation  $r$  of polymer chains using the Monte Carlo method [7,8]. However, energy contribution to elastic force is ignored in those investigations. In fact, energy change always exists in the process of tensile elongation. For example, the average energy per bond is about 1000 J/mol for polymethylene chain at 413 K [9], however, the average energy per bond is almost close to zero at the ultimate tensile elongation because all rotation states are almost in the *trans* conformations when  $\lambda = \lambda_{\max}$ . Therefore, energy contribution to elastic force should be considered [10–13]. We all know that the number of conformations for long polymer chains is very large, so it is difficult to study the statistical properties of polymer chains using the enumeration calculation method, especially for long polymer chains. The Monte Carlo (MC) method is widely used in studying the statistical properties, as well as the elastic behaviors of polymer chains [11,14–17]. In this paper, we use the MC method to get a great deal of poly(ethylene terephthalate) (PET) chains with different repeat units, then investigate the elastic behavior of PET chains with considering the rotational isomeric state model, especially discuss the energy and entropy contributions to elastic force. Of course, the statistical properties such as the dimensions and interior conformations of PET chains are also discussed here.

## 2. Method of calculation

The rotational-isomeric-state (RIS) model of Williams and Flory for PET chain is adopted here [18]. The *trans*- and *cis*-isomers of 6-bond repeat unit structure are shown in Fig. 1. Here  $l_i$  is the bond length, and  $\theta_i$  represents the valence angle supplement. The geometrical parameters taken from Williams and Flory [18,19], are as follows:  $l_1 = l_3 = l_{OC'} = 0.134$  nm ( $C'$  denotes the carbonyl carbon atom),  $l_4 = l_6 = l_{O-C} = 0.144$  nm,  $l_5 = l_{C-C} = 0.153$  nm,  $l_2 = 0.574$  nm (virtual bond),  $\theta_1 = \theta_2 = 66^\circ$ ,  $\theta_3 = \theta_6 = 67^\circ$ , and  $\theta_4 = \theta_5 = 70^\circ$ , respectively.

According to Flory's RIS model of PET chain, the statistical weight,  $u_{\zeta\eta;i}$ , associated with a rotational state  $\eta$  of skeletal bond  $i$  is also dependent upon the state  $\zeta$  at bond  $i-1$ , and the value is related to the corresponding rotational energy,  $E_{\zeta\eta;i}$ , as follows:

$$u_{\zeta\eta;i} = \exp\left(-\frac{E_{\zeta\eta;i}}{RT}\right) \quad (1)$$

here  $R$  is the gas constant and  $T$  is the absolute temperature. The statistical weights matrices for the six skeletal

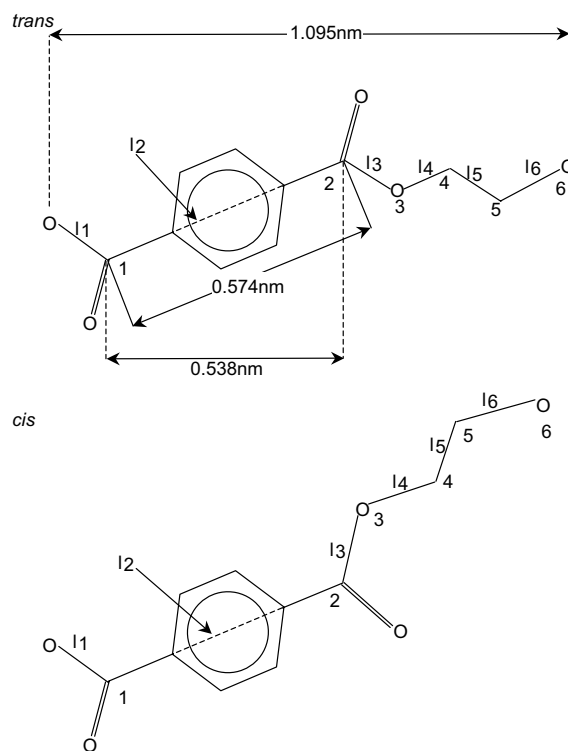


Fig. 1. *Trans*- and *cis*-PET repeat-unit structures, skeletal atoms are labelled 1–6, and bond lengths are denoted  $l_i$ .

bonds of the PET repeat unit (Fig. 1) are listed in the following equations [17]:

$$U_i = \begin{bmatrix} g_- & t & g_+ \\ g_- & & \\ t & & \\ g_+ & & \end{bmatrix}; \quad i \neq 2, 3;$$

$$U_2 = \begin{bmatrix} & cis & trans \\ g_- & & \\ t & & \\ g_+ & & \end{bmatrix} \quad U_3 = \begin{bmatrix} & g_- & t & g_+ \\ cis & & & \\ trans & & & \end{bmatrix}$$

$$U_1 = \begin{bmatrix} 0 & 1 & 0 \\ 0 & 1 & 0 \\ 0 & 1 & 0 \end{bmatrix} \quad (2)$$

$$U_2 = \begin{bmatrix} 0 & 0 \\ 1 & 1 \\ 0 & 0 \end{bmatrix} \quad (3)$$

$$U_3 = \begin{bmatrix} 0 & 1 & 0 \\ 0 & 1 & 0 \end{bmatrix} \quad (4)$$

$$U_4 = \begin{bmatrix} 0 & 0 & 0 \\ \sigma_4 & 1 & \sigma_4 \\ 0 & 0 & 0 \end{bmatrix} \quad (5)$$

$$U_5 = \begin{bmatrix} \sigma_5 & 1 & \sigma_5\omega \\ \sigma_5 & 1 & \sigma_5 \\ \sigma_5\omega & 1 & \sigma_5 \end{bmatrix} \quad (6)$$

$$U_6 = \begin{bmatrix} \sigma_6 & 1 & \sigma_6\omega \\ \sigma_6 & 1 & \sigma_6 \\ \sigma_6\omega & 1 & \sigma_6 \end{bmatrix} \quad (7)$$

In this model, the rotational angles of gauche conformational states of bonds 4–6 are at  $\Phi_{g\pm} = \pm 120^\circ$ . Here  $\sigma_i = \exp(-E_i/RT)$ , and  $\omega = \exp(-E_\omega/RT)$ , and the energies associated with the statistical weights  $\sigma_4$ ,  $\sigma_5$ ,  $\sigma_6$ , and  $\omega$ , are  $E_{\sigma 4} = E_{\sigma 6} = 1.75 \text{ kJ mol}^{-1}$ ,  $E_{\sigma 5} = -4.16 \text{ kJ mol}^{-1}$  and  $E_\omega = 5.80 \text{ kJ mol}^{-1}$  [17]. In this paper, all properties are discussed at  $T = 523 \text{ K}$ .

It is well known that the appearance probabilities of the states  $g^-$ ,  $t$  and  $g^+$  are related to the above six statistical weights matrices  $U_i = [u_{\zeta\eta;i}]$ . According to these matrices, we can get the corresponding probabilities matrices  $P_i = [p_{\zeta\eta;i}]$ . From  $U_1$  to  $U_3$ , the statistical weights are all equal to zero except for  $\zeta = \eta = t$ . That means in one repeat unit from the first atom to the third atom all fall in *trans* state, and  $P_1 \sim P_3$  only has the a priori probability  $p_{tt} = 1.0$ , while the a priori probability  $p_{\zeta\eta;i}$  of relevant bond pairs in states  $\zeta\eta$  is defined by [9]

$$p_{\zeta\eta;i} = (n-2)^{-1} \frac{\partial \ln Z}{\partial u_{\zeta\eta;i}} \quad (i = 4, 5, 6) \quad (8)$$

The results of  $n = 180$  ( $x = 30$  repeat unit) of PET chains are listed here:

$$P_i = \begin{bmatrix} & g^- & t & g^+ \\ g^- & & & \\ t & & & \\ g^+ & & & \end{bmatrix} \quad (i = 4, 5, 6)$$

$$P_4 = \begin{bmatrix} 0 & 0 & 0 \\ 0.2424 & 0.5152 & 0.2424 \\ 0 & 0 & 0 \end{bmatrix} \quad (9)$$

$$P_5 = \begin{bmatrix} 0.1385 & 0.0674 & 0.0365 \\ 0.2072 & 0.1008 & 0.2072 \\ 0.0365 & 0.0674 & 0.1385 \end{bmatrix} \quad (10)$$

$$P_6 = \begin{bmatrix} 0.1385 & 0.2072 & 0.0365 \\ 0.0674 & 0.1008 & 0.0674 \\ 0.0365 & 0.2072 & 0.1385 \end{bmatrix} \quad (11)$$

In our Monte Carlo procedure, we use a computer simulated random process to produce a random number,

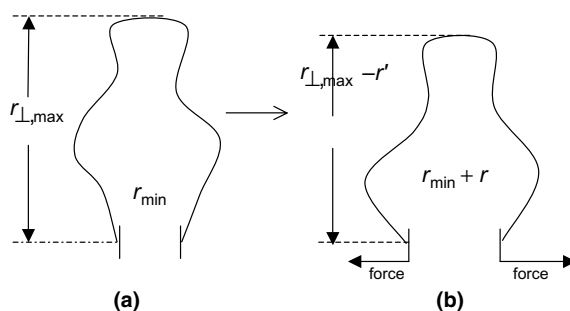


Fig. 2. Conformations of an isolated chain (a) and of a chain with a force acting on (b). The minimum of the end-to-end distance increases from  $r_{\min}$  to  $r_{\min} + r$  in the process of tensile elongation.

and the  $i$ th atom's position depends on the position of the  $(i-1)$ th atom and the probability of  $p_{\zeta\eta;i}$ .

When a force  $f$  acts on the PET chains, the atoms in the PET chains elongate the distance  $r$  along the force direction, while compressed and drawn back  $r'$  in the vertical of the force direction, and a lot of conformations would vanish. If the force  $f = 0$ , this is the isolated chain, and the minimum of the end-to-end distance is  $r_{\min}$  (see Fig. 2(a)). If  $f \neq 0$ , the minimum of the end-to-end distance becomes  $r_{\min} + r$  (see Fig. 2(b)). If we assume that the force  $f$  is in the direction of the  $x$ -axis, the partition function of the system is:

$$Z(r) = \sum_i \exp(-E_i/RT) \quad (12)$$

here  $\sum_i$  is the sum of the conformations whose  $x$ -axis component of end-to-end distance is greater than  $r$ , meanwhile the  $y$ - and  $z$ -axis components of end-to-end distance are less than  $r_{y,\max} - r'$  and  $r_{z,\max} - r'$ , respectively. Of course, it is very difficult to calculate the partition function of long PET chains according to Eq. (12) as the number of conformations is very large. Here we introduce the parameter of the distribution probability  $P_x(r)$ , and the distribution probability  $P_x(r)$  with the  $x$ -axis component of end-to-end distance is greater than  $r$ , meanwhile the  $y$ - and  $z$ -axis components of end-to-end distance are less than  $r_{y,\max} - r'$  and  $r_{z,\max} - r'$ , can also be obtained from following equation:

$$P_x(r) = \frac{\sum_i \exp(-E_i/RT)}{Z} = \frac{Z(r)}{Z} \quad (13)$$

where  $Z$  is the partition function without elongation, and can be obtained from successional multiple of the statistical weights matrices [9]. If we can know distribution probability  $P_x(r)$ , we can obtain  $Z(r)$  exactly from Eq. (13). Here we use Monte Carlo simulation method to calculate the distribution probability  $P_x(r)$ . In our Monte Carlo simulation,  $C_S$  is the number of samples

and  $C_x$  is the number of samples whose  $x$ -axis component of end-to-end distance is greater than  $r$ , meanwhile the  $y$ - and  $z$ -axis components of end-to-end distance are less than  $r_{y,\max} - r'$  and  $r_{z,\max} - r'$ , respectively. Therefore, distribution probability  $P_x(r)$  is

$$P_x(r) = \frac{C_x}{C_s} \quad (14)$$

So the partition function  $Z(r)$  is

$$Z(r) = Z \times \frac{C_x}{C_s} \quad (15)$$

Deformation along one of the axes independently decreases the number of chain conformation. The elongation ratio  $\lambda_e$  and the compression ratio  $\lambda_c$  are obtained from the root-mean-square of end-to-end distance  $\langle R^2 \rangle_0^{1/2}$  of PET chains without deformation:

$$\lambda_e = \frac{\langle R^2 \rangle_0^{1/2} + r}{\langle R^2 \rangle_0^{1/2}} \quad \lambda_c = \frac{\langle R^2 \rangle_0^{1/2} - r'}{\langle R^2 \rangle_0^{1/2}} \quad (16)$$

In this paper, we only consider the case of simple elongation  $\lambda_x = \lambda_e = \lambda$ , and  $\lambda_y = \lambda_z = \lambda_c = \lambda_e^{-1/2} = \lambda^{-1/2}$ . From the partition function, we can derive the average free energies of PET chains under various elongation ratios  $\lambda$

$$\langle A \rangle = -RT \ln Z(r) \quad (17)$$

$$\langle U \rangle = \frac{RT^2}{Z(r)} \frac{dZ(r)}{dT} \quad (18)$$

In the meantime, elastic force  $f$  can be obtained from the dependence of  $\langle A \rangle$  on the elongated distance along the force direction [2,11–13]:

$$f = \frac{\partial \langle A \rangle}{\partial r} \quad (19)$$

According to Newton's third law, the force  $f$  is the elastic force stored in the polymer chains. The energy elastic contribution to the elastic force  $f_U$  is also defined by

$$f_U = \frac{\partial \langle U \rangle}{\partial r} \quad (20)$$

We know  $\langle A \rangle = \langle U \rangle - TS$ , so we can also calculate the entropy contribution to the elastic force  $f_S$

$$f_S = \frac{\partial (-TS)}{\partial r} = f - f_U \quad (21)$$

### 3. Results and discussion

#### 3.1. Average conformations of PET chains

In order to find out the interior conformation changes in the process of tensile elongation, we first calculate the a priori probabilities for bonds 4–6, and the results are shown in Fig. 3. Here the number of repeat

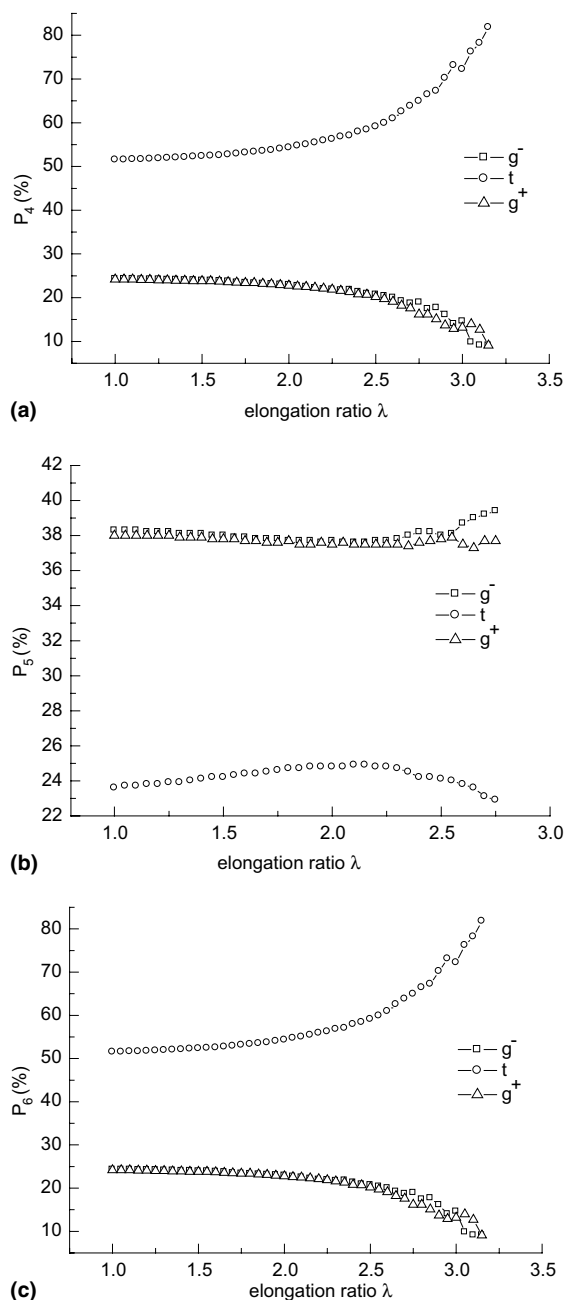


Fig. 3. The probabilities of rotational states of three consecutive bonds  $P_4$ – $P_6$  as a function of elongation ratio  $\lambda$  with chain length of  $n=60$  bonds (10 repeat units).

unit of PET chain is  $x=10$  (the number of bonds of PET chain is 60). The probability  $P_{\eta;i}$  is defined by the following equation:

$$P_{\eta;i} = \sum_{\zeta=g^-,t,g^+} p_{\eta;\zeta;i} \quad (i=4,5, \text{ or } 6) \quad (22)$$

From these curves, we can obtain much significant information. The situations of  $P_4$  and  $P_6$  are very similar in Fig. 3(a) and (c). The probability of state  $t$  are far greater than that of state  $g^-$  or  $g^+$ , and almost close to twice as large as state  $g^-$  or  $g^+$ . The difference between states  $g^-$  and  $g^+$  is not very obvious here. Furthermore the value of  $P_{t;4}$  (or  $P_{t;6}$ ) increases slowly with  $\lambda$  at small elongation ratio  $\lambda$ , however, it increases relatively fast with  $\lambda$  when  $\lambda > 2.50$ . In the meantime,  $P_{g^-;4}$  (or  $P_{g^+;4}$ ), or  $P_{g^-;6}$  (or  $P_{g^+;6}$ ) reduces slowly at the beginning of tensile elongation and decreases relatively fast when  $\lambda > 2.50$ . However, the relative different behavior is obtained in Fig. 3(b). In Fig. 3(b), the value of  $P_{g^-;6}$ , (or  $P_{g^+;6}$ , or  $P_{t;6}$ ) changes a little in the process of tensile elongation. For example,  $P_{t;6}$  increases a little in the region of  $\lambda > 2.2$ , and decreases slowly when  $\lambda > 2.2$ . Through our calculations, we can know the changes of the interior conformations of PET chains clearly. Therefore, we can make the conclusion that in one PET repeat unit, the 4th and 6th bonds tend to be in the state  $t$  while the 5th bond inclines to be the state  $g^-$  or  $g^+$  in the process of tensile elongation.

The mean-square end-to-end distance  $\langle R^2 \rangle$  and the mean-square radius of gyration  $\langle S^2 \rangle$  are also investigated here, and the results are given in Figs. 4 and 5. In Fig. 4, the characteristic ratio of the mean-square end-to-end distance  $\langle R^2 \rangle_0 / nl_0^2$  without elongation is 3.03 for  $n = 180$  ( $x = 30$ ), which is close to the theoretical result of  $(\langle R^2 \rangle_0 / nl_0^2)_\infty = 3.10$ . In the process of tensile elongation, the characteristic ratio of mean-square end-to-end distance  $\langle R^2 \rangle_\lambda / nl_0^2$  increases with elongation ratio  $\lambda$ . In Fig. 5, we also plot the ratio of  $\langle R^2 \rangle / \langle S^2 \rangle$  as a function of elongation ratio  $\lambda$ . For an isolated PET chain ( $\lambda = 1.0$ ), the ratio of  $\langle R^2 \rangle / \langle S^2 \rangle$  is 6.67, 6.37, and 6.29 for  $n = 60$  ( $x = 10$ ), 120 ( $x = 20$ ), and 180 ( $x = 30$ ), respectively, which is greater than that of random walk-

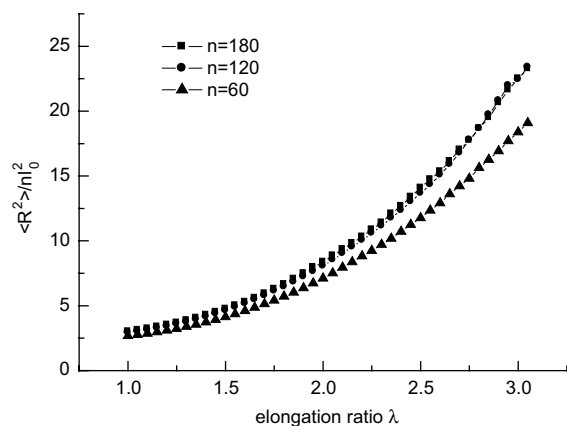


Fig. 4. Characteristic ratio of mean-square end-to-end distance  $\langle R^2 \rangle / nl_0^2$  as a function of elongation ratio  $\lambda$  for PET chains with chain length of  $n = 60, 120$ , and  $180$  bonds. Here  $l_0^2 = (l_1^2 + l_2^2 + l_3^2 + l_4^2 + l_5^2 + l_6^2) / 6$ .

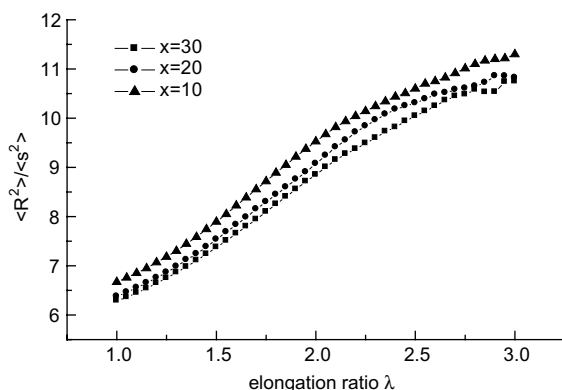


Fig. 5. The ratio of  $\langle R^2 \rangle / \langle S^2 \rangle$  as a function of elongation ratio  $\lambda$  for PET chain with  $x = 10, 20$ , and  $30$  repeat units.

ing chain [20]. Of course, if the PET chain is long enough, the ratio of  $\langle R^2 \rangle / \langle S^2 \rangle$  may be close to 6.0 of random walking chain. When the force  $f$  acts on the PET chains, the chains are elongated along the force direction, and become more flat shapes. This leads the value of  $\langle R^2 \rangle / \langle S^2 \rangle$  to increase.

In order to investigate the shape of PET chains in the tensile elongation in more detail, here we consider the radius of gyration tensor  $S$ , defined as:

$$S = \frac{1}{n+1} \sum_{i=0}^n S_i S_i^T = \begin{pmatrix} S_{xx} & S_{xy} & S_{xz} \\ S_{yx} & S_{yy} & S_{yz} \\ S_{zx} & S_{zy} & S_{zz} \end{pmatrix} \quad (23)$$

Here  $S_i = \text{col}(x_i, y_i, z_i)$  is the position of atom  $i$  in a frame of reference with its origin at the center of mass. The tensor  $S$  can be diagonalized to form a diagonal matrix with three eigenvalues  $L_1^2$ ,  $L_2^2$  and  $L_3^2$  ( $L_1^2 \leq L_2^2 \leq L_3^2$ ). Solc and Stockmayer first used  $\langle L_1^2 \rangle : \langle L_2^2 \rangle : \langle L_3^2 \rangle$  to measure the shape of flexible polymer chains [21,22], and they estimated the ratio to be 1:2.7:11.7 based on a random walk of 100 bonds on a simple cubic lattice using Monte Carlo (MC) technique [21,22]. Here we get the ratios of 1:3.7:19.2, 1:3.2:15.7 and 1:3.1:14.6 for 10-, 20- and 30-repeat-unit PET chains without elongation, and all greater than that of random walking chains. The reason may be that the number of bonds is not large enough. In Fig. 6, we find the tendency of  $\langle L_2^2 \rangle / \langle L_1^2 \rangle$  and  $\langle L_3^2 \rangle / \langle L_1^2 \rangle$  for PET chain without elongation ( $\lambda = 1.0$ ) is close to 2.7 and 11.7, respectively when PET chains become long enough. In the process of tensile elongation, we find the behaviors of  $\langle L_2^2 \rangle / \langle L_1^2 \rangle$  and  $\langle L_3^2 \rangle / \langle L_1^2 \rangle$  are different. In Fig. 6(a),  $\langle L_2^2 \rangle / \langle L_1^2 \rangle$  increases with elongation ratio  $\lambda$  in the region of  $\lambda = 1.0$ –2.5, then decreases with elongation ratio  $\lambda$  when  $\lambda > 2.5$ . However, in Fig. 6(b),  $\langle L_3^2 \rangle / \langle L_1^2 \rangle$  increases with elongation ratio, especially for  $n = 60$ , here  $n$  is the number of bonds of PET chains. It is visually pictured as a 3D-globe in Fig. 6(a) that when we act a force along the direction of  $\langle L_3^2 \rangle$ , the directions of  $\langle L_2^2 \rangle$

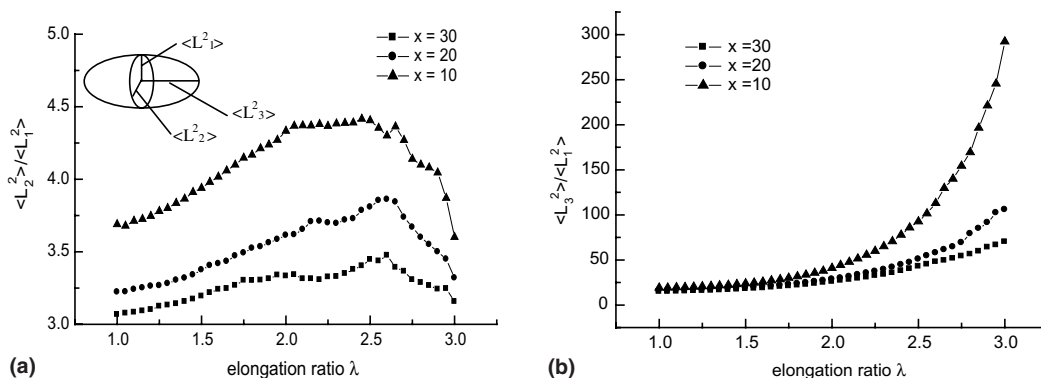


Fig. 6. The ratios of  $\langle L_2^2 \rangle / \langle L_1^2 \rangle$  and  $\langle L_3^2 \rangle / \langle L_1^2 \rangle$  as a function of elongation ratio  $\lambda$  for PET chain with  $x=10, 20$ , and  $30$  repeat units.

and  $\langle L_1^2 \rangle$  compress accordingly. In Fig. 6(a), when the elongation ratio  $\lambda$  2.5,  $\langle L_2^2 \rangle$  changes faster than  $\langle L_1^2 \rangle$ , therefore, this leads the ratio of  $\langle L_2^2 \rangle / \langle L_1^2 \rangle$  to increase. However, when  $\lambda > 2.5$ ,  $\langle L_2^2 \rangle$  changes slower than  $\langle L_1^2 \rangle$ , and this leads the ratio of  $\langle L_2^2 \rangle / \langle L_1^2 \rangle$  to decrease. So we can find the tendency of ratio of  $\langle L_2^2 \rangle / \langle L_1^2 \rangle$  in Fig. 6(a). PET is not very symmetrical molecule so different directions have different reactions to the force. When  $n=60$  ( $x=10$ ), the ratio of  $(\langle L_3^2 \rangle / \langle L_1^2 \rangle)_{\max} : (\langle L_3^2 \rangle / \langle L_1^2 \rangle)_{\min}$  is close to 15.22. However, when  $n=180$  ( $x=30$ ), the ratio of  $(\langle L_3^2 \rangle / \langle L_1^2 \rangle)_{\max} : (\langle L_3^2 \rangle / \langle L_1^2 \rangle)_{\min}$  decreases to 4.78. In a word, the shape of PET chain becomes flat in parallel to the direction of force in the process of tensile elongation.

### 3.2. Thermodynamics properties of PET chains

In fact, energy changes always exist in the process of tensile elongation. The changes of average conformations lead to change of thermodynamics properties of PET chains. Here we first calculate the average energy and the average free energy per repeat unit according to Eqs. (17) and (18), and the results are shown in Figs. 7 and 8, respectively. In our Monte Carlo simulation,  $C_S$ , the number of samples, is equal to 10,000,000.

The average energies per repeat unit decrease with elongation ratio  $\lambda$  and the value of 30-repeat-unit PET chain is greater than that of 20-repeat-unit (or 10-repeat-unit) PET chains with the same elongation ratio  $\lambda$  in Fig. 7. When elongation ratio  $\lambda$  reaches to the range of 2.45–2.55, the curves fall down much evidently. In the Gaussian or non-Gaussian chain model of rubber elasticity [2], it is supposed that the change of energy is zero ( $\Delta U=0$ ) in the calculation of shear stress. We find out that the change of energy ( $\Delta U$ ) is small for small-scale deformation, especially for long PET chains, indicating the agreement between the theoretical curve of the Gaussian chain model and the experimental curve for small elongation [2,23]. But for large-scale deformation, the average energies abruptly decrease with elonga-

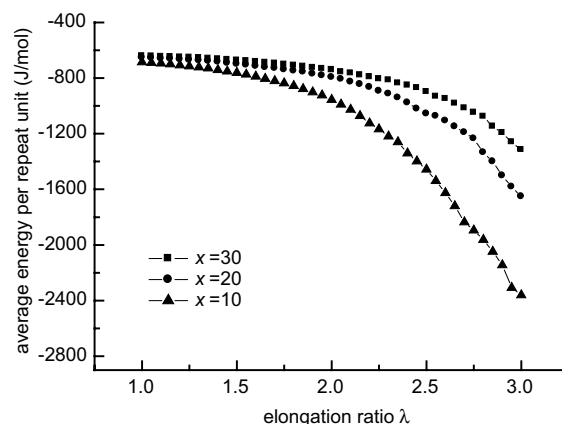


Fig. 7. Average energy per repeat unit  $\langle U \rangle$  as a function of elongation ratio  $\lambda$  for PET chains with  $x=10, 20$ , and  $30$  repeat units.

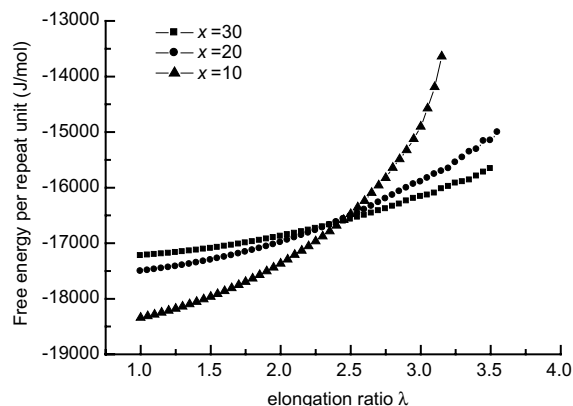


Fig. 8. Average free energy per repeat unit  $\langle A \rangle$  as a function of elongation ratio  $\lambda$  for PET chains with  $x=10, 20$ , and  $30$  repeat units.



tion ratio  $\lambda$ , and this may be the reason why there are large deviations between the theoretical and experimental results [2,23].

The average free energies per repeat unit in Fig. 8 are contrary to the above average energies, and increase with elongation ratio  $\lambda$ . The curve of short PET chains is less than that of long PET chains in the region of small elongation ratio  $\lambda$ , and greater than that of long PET chains in the region of large elongation ratio  $\lambda$ . In the region  $\lambda=2.45\text{--}2.55$ , the average free energies per repeat unit for different chain lengths are almost the same.

According to Eqs. (19) and (20), the elastic force stored in the PET chains can be calculated. As elastic force  $f$  is the free energy's derivative with respect to  $r$ , so Eqs. (19) and (20) could be rewritten as [24,25]:

$$f = \lim_{\Delta r \rightarrow 0} \frac{\Delta \langle A \rangle}{\Delta r} \quad (24)$$

$$f_U = \lim_{\Delta r \rightarrow 0} \frac{\Delta \langle U \rangle}{\Delta r} \quad (25)$$

In our calculation,  $\Delta r = 0.05 \times \langle R^2 \rangle_0^{1/2}$ , and the results are shown in Figs. 9–11.

In Fig. 9, the elastic force per repeat unit increases with elongation ratio  $\lambda$  for different PET chains. The elasticity ties in the length of the spring and stores in the spring chains naturally; the elastic force increases with elongation certainly. At the same time, the energies contribution to elastic force  $f_U$  is shown in Fig. 10. The value of  $f_U$  is all less than zero. For small elongation ratio  $\lambda$ ,  $f_U$  decreases gradually with elongation ratio  $\lambda$ , but fluctuate remarkably for large elongation ratio  $\lambda$ , especially for short PET chains. On the one hand, the number of bonds is too small to affect the statistical results; on the other hand, just like the spring, elongation ratio  $\lambda$  is too big to destroy the elastic of the polymer chains and that brings the fluctuation of  $f_U$ .

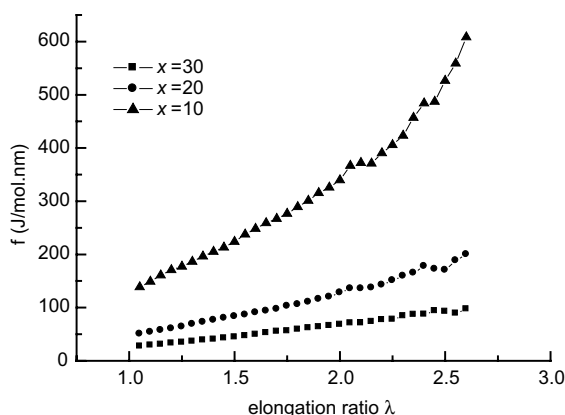


Fig. 9. Elastic force per repeat unit  $f$  as a function of elongation ratio  $\lambda$  for PET chains with  $x=10, 20$ , and  $30$  repeat units.

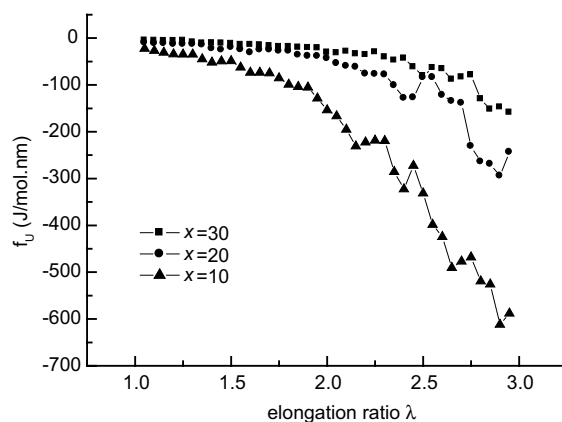


Fig. 10. Energy contribution to elastic force per repeat unit  $f_U$  as a function of elongation ratio  $\lambda$  for PET chains with  $x=10, 20$ , and  $30$  repeat units.

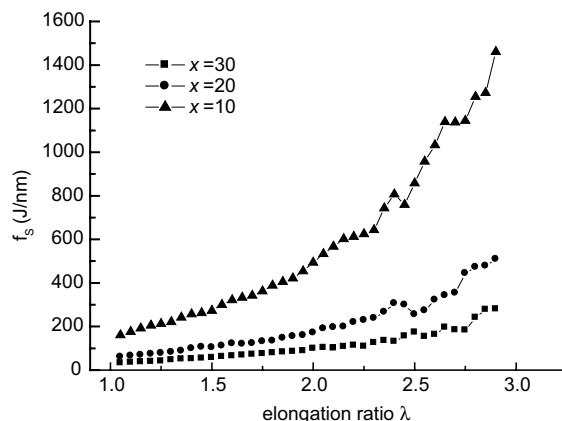


Fig. 11. Entropy contribution to elastic force per repeat unit  $f_S$  as a function of elongation ratio  $\lambda$  for PET chains with  $x=10, 20$ , and  $30$  repeat units.

From the knowledge of thermodynamic statistical physics, we all know Eq. (26):

$$\langle A \rangle = \langle U \rangle - TS \quad (26)$$

Here  $S$  is the entropy of PET chains. From the force  $f$  and the energies contribution to elastic force  $f_U$ , we can know that the entropy contribution to elastic force  $f_S$  can be written as:

$$f_S = f - f_U, \quad (27)$$

In Fig. 11, we plot the entropy contribution to elastic force  $f_S$  as a function of elongation ratio  $\lambda$ . Here the curve is similar to the elastic force  $f_U$ , and entropy  $S$  indicates the chaos degree of the system, so the PET chains tend to be disordered with elongation ratio  $\lambda$ , especially for short PET chains.

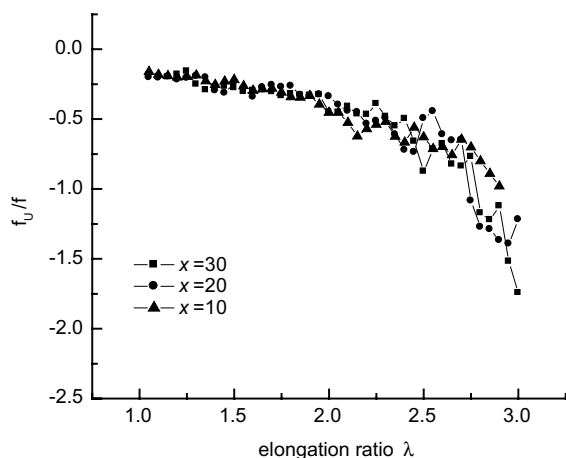


Fig. 12. The ratio  $f_u/f$  as a function of elongation ratio  $\lambda$  for PET chains with  $x=10, 20$ , and  $30$  repeat units.

The ratio  $f_u/f$  is also calculated, and the results are given in Fig. 12. We find that the ratio  $f_u/f$  decreases with  $\lambda$ , and the ratio is less than zero and almost independent of chain length. In fact,  $f_u/f$  can be obtained by experimental method, therefore, the ratio  $f_u/f$  is an important parameter in statistical properties of polymer chains. Those investigations may provide some insights into the macroscopic phenomena of rubber elasticity.

### Acknowledgments

The research was financially supported by National Natural Science Foundation of China (nos. 29874012, 20174036, 20274040), and Natural Science Foundation of Zhejiang Province (no. 10102).

### References

- [1] Treloar LRG. The physics of rubber elasticity. 3rd ed. Oxford, UK: Clarendon Press; 1975.
- [2] Flory PJ. Principles of polymer chemistry. Ithaca, New York: Cornell University Press; 1953.
- [3] Mark JE, Erman B. Rubberlike elasticity: a molecular primer. New York: Wiley-Interscience; 1988.
- [4] Kuhn W, Guth E. Kolloid-Z 1942;101:248–51.
- [5] Treloar LRG. Trans Faraday Soc 1946;42:77–94.
- [6] Abe Y, Flory PJ. J Chem Phys 1970;52:2814–20.
- [7] Mark JE, Curro JG. J Chem Phys 1983;79:5705–9.
- [8] Curro JG, Mark JE. J Chem Phys 1984;80:4521–5.
- [9] Flory PJ. Statistical mechanics of chain molecules. New York: Wiley-Interscience; 1969.
- [10] Yang XZ, Li XF. Chin J Polym Sci 1998;16:279–82.
- [11] Zhang LX, Huang YX, Zhao DL. Macromol Theory Simul 2001;10:479–84.
- [12] Zhang LX, Xia AG, Jiang ZT, Zhao DL. Macromol Theory Simul 2001;10:651–5.
- [13] Zhang LX, Jiang ZT, Zhao DL. J Polym Sci Part B: Polym Phys 2002;40:105–14.
- [14] Stepto RFT, Taylor DJR. J Chem Soc Faraday Trans 1995;91:2639–48.
- [15] Taylor DJR, Stepto RFT, Jones RA, Ward IM. Macromolecules 1999;32:1978–89.
- [16] Cail JI, Taylor DJR, Stepto RFT, Brereton MG, Jones RA, Ries ME, et al. Macromolecules 2000;33:4966–71.
- [17] Cail JI, Stepto RFT. Polymer 2003;44:6077–87.
- [18] Williams AD, Flory PJ. J Polym Sci Part A-2 1967;5: 417–26.
- [19] Zhen X, Sun J. J Polym Sci Part B: Polym Phys 2002;40: 2646–52.
- [20] Yamakawa H. Modern theory of polymer solutions. New York: Interscience; 1971.
- [21] Solc K, Stockmayer WH. J Chem Phys 1971;54:2756.
- [22] Solc K. J Chem Phys 1971;55:335–44.
- [23] Treloar LRG. Trans Faraday Soc 1943;39:241–8.
- [24] Sun J, Yang XZ. Chin J Polym Sci 2001;19:447–9.
- [25] Sun J, Yang XZ. Chin Sci Bull 2002;47:1794–6.